The thorium-229 low-energy isomer and the nuclear clock

Kjeld Beeks[1], Tomas Sikorsky[1], Thorsten Schumm[1], Johannes Thielking[2], Maxim V. Okhapkin[2], Ekkehard Peik[2]*

[1] Vienna Center for Quantum Science and Technology, Atominstitut, TU Wien, Stadionallee 2, 1020 Vienna, Austria

[2] Physikalisch-Technische Bundesanstalt, 38116 Braunschweig, Germany

*e-mail: ekkehard.peik@ptb.de

Abstract

The ^{229}Th nucleus is known to possess an isomeric state at an energy of about 8 eV above the ground state, several orders of magnitude lower than typical nuclear excitation energies. This has inspired a field of low-energy nuclear physics where nuclear transition rates will be influenced by the electron shell. The low energy makes the ^{229}Th isomer accessible to resonant laser excitation. Realized with laser-cooled trapped thorium ions or with thorium dopant ions in a transparent solid, the nuclear resonance may serve as the reference for an optical clock of very high accuracy. Precision frequency comparisons between such a nuclear clock and conventional atomic clocks will provide sensitivity to effects of hypothetical new physics beyond the standard model. While laser excitation of ^{229}Th remains an unsolved challenge, recent experiments have provided essential information on the transition energy and relevant nuclear properties.

1. Introduction and Motivation

While we are used to speak about *atomic* clocks, the origin of these devices can be traced to research on *nuclear* physics. In 1924 W. Pauli pointed out that some splittings of atomic spectral lines originate from the coupling between the magnetic moments of the nucleus and the electrons[1]. In 1935 H. Casimir showed that a related effect with a different spectral pattern is produced by the electric interaction when the charge distribution of the nucleus is not spherically symmetric[2]. Based on precision measurements of this hyperfine structure, spectroscopy of atomic transitions became an important source of information on nuclear properties. The group of I. Rabi at Columbia University investigated atomic beams interacting with microwave radiation[3]. Some of the resonances could be recorded with such excellent reproducibility that Rabi proposed in 1945 to use them in "the most accurate of timepieces"[4]. This was the seminal idea for the cesium atomic clock that serves as the basis of time keeping until today[5]. While the fields of atomic and nuclear physics expanded in diverse directions in the second half of the 20th century, we now see an emerging topic that creates new links between both domains. Again, the concept of a highly precise clock plays the central role.

The resonance frequency of the Cs clock at about 9.2 GHz is determined by the properties of the ^{133}Cs nucleus, the valence electron, and their electromagnetic interactions. In a well-designed clock, the atoms are protected from external perturbations that would otherwise shift the resonance frequency. In recent years, much progress towards more accurate

clocks has been obtained in optical clocks[6] that make use of resonance frequencies of transitions in the atomic electron shell in the optical frequency range ($\approx 10^{15}$ Hz). Reaching trailblazing accuracies in the 10^{-18} range (comparable to missing 1 s over the age of the universe), it is critical to control all interactions of the atom with the environment, for example, the thermal radiation emitted by surfaces surrounding the atoms. The aspect of finding a reference oscillator that is less sensitive to external fields has motivated the concept of an optical nuclear clock, first proposed in 2003[7]. The small size of the nucleus and tight binding of its constituents makes resonant frequencies associated with internal excitations highly insensitive to external fields[7,8]. But the strong binding inside the nucleus also places the characteristic energies for electromagnetic transitions in the $0.1 - 1$ MeV range, orders of magnitude above the photon energies used in current atomic clocks.

Fortunately, nature has provided a system for developing a nuclear clock in the optical frequency range: the low-energy isomer in ^{229}Th (Refs. [9–11]). The ^{229}Th nucleus is unique in nuclear physics providing the only isomer energy in the range of outer-shell electronic transitions. In addition to its relevance for the nuclear clock, this opens a field of low-energy nuclear physics for experimental studies, where nuclear and electronic excitations can couple because they appear in the same energy range [12–14]. A main experimental challenge is to drive this nuclear excitation resonantly with a narrow-band tunable laser. This quest has largely motivated the developments of the nuclear clock and it is the goal of several ongoing experiments[10,11].

In this Perspective we will review recent research activities on the ^{229}Th low-energy isomer that have resulted in novel experimental methods and insights in the properties of the nucleus, together with a steady stream of ideas for further research and applications. Earlier and contemporary reviews of the field can be found in[10,11,15-17].

2. Thorium-229 properties, production and sample preparation

^{229}Th is a radio-isotope (see Fig. 1): it has a half-life of $T_{1/2} = 7917(24)$ years, decays through α-decay (100%) with $Q_\alpha = 5168$ keV[18]. Due to the short half-life, ^{229}Th is not primordial; it has to be actively produced in nuclear

decay or fission processes. The current global stock is derived from man-made ^{233}U (about 1 ton, bred in nuclear reactors during the Cold War). It is estimated to 750 grams, out of which about 40 grams have sufficient isotopic purity[19,20]. Production through other isotopes is being investigated due to renewed interest in ^{229}Th for medical applications[21].

The spin and parity of the ^{229}Th nuclear ground state have been determined to be $I^\pi = 5/2^+$ [22,23], the isomeric state was assigned $I^\pi = 3/2^+$ [24] and experimentally verified in[25]. The magnetic dipole (μ) and the spectroscopic electric quadrupole moments (Q_s) are $\mu = 0.360(7)$ μ_N and $Q_s = 3.11(6)$ eb for the ground state[26] and $\mu = -0.37(6)$ μ_N and $Q_s = 1.74(6)$ eb for the isomeric state, respectively[25]. Measurements of the isomer energy and other nuclear structure properties are described in detail in section 3.

Fig. 1 | Section of the table of nuclides showing the natural decay paths leading to the production of (isomeric) ^{229}Th: α-decay (yellow) of ^{233}U, β^--decay (green) of ^{229}Ac, β^+-decay of ^{229}Pa (red).

The low-lying isomer energy emerges as the consequence of a very fine interplay between the nuclear rotation-vibration degrees of freedom and their coupling to the motion of the unpaired neutron (see Fig. 2). The radiative nuclear transition from the isomer to the ground state is predicted to be of mixed magnetic dipole (M1) and electric quadrupole (E2) character[27] resulting in a lifetime in the range of 10^4 s.

If energetically possible, transfer of the isomer excitation energy to an electron from the shell proceeds much faster than radiative decay and an internal conversion lifetime of 7 μs has been observed for neutral Th (Ref. [28]).

Three nuclear decay processes lead into ^{229}Th: α-decay of ^{233}U, β-decay of ^{229}Ac, and electron capture decay of ^{229}Pa (see Fig. 1). α-decay of ^{233}Uranium ($T_{1/2}$ = 1.6 × 10^5 years) is currently the only means to obtain significant quantities of ^{229}Th. An energy of Q_α = 4909 keV is released in the α-decay, transferring a recoil energy of 84 keV onto the ^{229}Th nucleus. This energy is sufficient to eject ^{229}Th recoil ions from thin layers (few tens of nm) of ^{233}U, which can be used to produce a ^{229}Th recoil ion source (see section 3). 2% of the ^{233}U α−decay events lead to a population of the low-energy ^{229}Th isomer[9,25,29,30]. This method has been the most successful way to produce isomeric ^{229}Th in a series of breakthrough experiments (see sections 3 and 4).

As an alternative, the β-decay of ^{229}Ac ($T_{1/2}$ = 62.7 min) can be used to produce (isomeric) ^{229}Th. ^{229}Ac undergoes 100% β-decay (Q_β = 1.1 MeV) to ^{229}Th, population of the ^{229}Th isomer is 14% < $\lambda_{\beta,isomer}$ < 94%, at least a factor 7 above the yield obtained in ^{233}U α-decay[31]. The recoil impacted on the ^{229}Th nucleus is at maximum 2.3 eV (Ref. [32]), below typical displacement

energies of solids. Production of ^{229}Ac in the ISOLDE facility has been demonstrated[33] and the use of ^{229}Ac to populate the ^{229}Th isomer and measure the isomer energy via direct radiative decay has been recently proposed[31].

^{229}Th is also obtained in electron capture decay of ^{229}Pa ($T_{1/2}$ = 1.5 days), however, on-line production of ^{229}Pa remains to be demonstrated. ^{229}Th can also be produced in radioactive beam facilities, like IGISOL, for example in a ^{232}Th(p,p3n)^{229}Th light ion-induced fusion-evaporation reaction, cross-sections for this reaction are currently being determined.

Two types of preparations of the nuclei are predominantly employed in experiments towards the use of ^{229}Th for a nuclear clock: Th atomic ions in radio frequency (RF) ion traps and Th-doped, optically transparent crystals. These systems are suitable for optical spectroscopy with a small number of nuclei of the rare isotope (extending to the extreme of working with a single trapped ion) and they permit to study the radiative excitation or decay of the isomer without energy transfer via the electron shell, as it would be the case in neutral Th atoms or thorium metal.
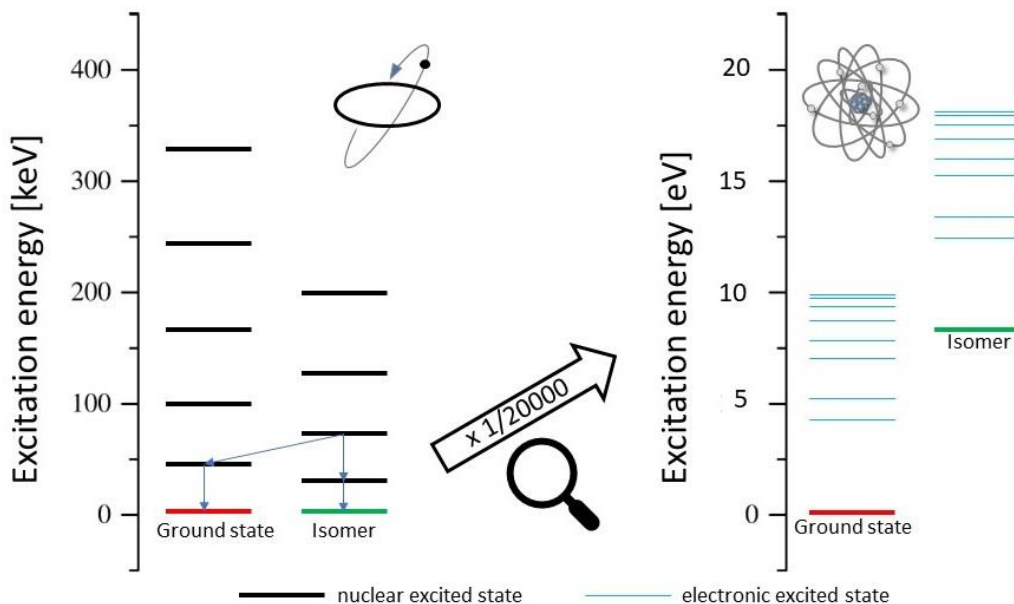

Fig. 2 | Schematic level schemes of ^{229}Th. Left: the overall nuclear level structure is determined by rotational bands. Ground state and isomer are the nearly degenerate heads to two different bands. Arrows indicate cascades of γ-transitions that have been used in the first measurements of the isomer energy. Right: On a 20000-times stretched energy scale the two lowest nuclear states together with their electronic level structure become visible. The electronic structure (shown here largely simplified) is like for an ion of Th$^+$.

Ion traps

Since their introduction in 1958, radio frequency traps have been used successfully to investigate the properties of ions isolated from environmental perturbations[34]. They are employed in some of the most accurate atomic clocks currently available, reaching fractional uncertainties on the order of 10^{-18} (Refs. [35,36]).

Several experiments have used linear RF traps to perform precision spectroscopy on thorium ions in various charge states (see, e.g., Refs. [37–39]). The charge states Th^+ and Th^{2+} have been employed to search for interactions between the electron shell and the nucleus. Having three and two valence electrons respectively, their dense electronic level structures are likely to interact with the low-lying nuclear transition (see Sec. 4). However, these charge states lack suitable closed electronic transitions for laser-cooling. Techniques like sympathetic laser cooling using a different ion of comparable charge to mass ratio[40] or buffer-gas cooling with a neutral atom or molecule[37] are therefore necessary. Buffer-gas cooling with a rare gas at room temperature is easy to implement but still leads to significant Doppler-broadening and a loss of Th ions through reactions with impurities in the background gas. Collisions with the buffer gas are also used to quench meta-stable states, which otherwise would need to be repumped with lasers[41].

The charge states Th^{3+} and Th^{4+} have been considered for the realization of the nuclear clock based on trapped ions[10]. The Th^{3+} ion possesses only one valence electron, facilitating the electronic state preparation to minimize the perturbation of the nuclear transition[7,8]. Although it has been shown that $^{229}Th^{3+}$ can be directly laser cooled[36], sympathetic cooling with another isotope[38] ($^{232}Th^{3+}$) or element[40] (e.g., Ca^+ or Sr^+) may be more convenient as it avoids optical pumping between multiple hyperfine sublevels.

Since the charge state Th^{4+} has a Rn-like closed shell of valence electrons, it is expected to be even less sensitive to external perturbations, although effects like Sternheimer antishielding need to be considered[42]. The closed electron shell also doesn't offer suitable transitions for laser cooling and hyperfine spectroscopy, requiring methods like quantum logic spectroscopy[43] with an auxiliary ion for cooling and readout of the nuclear state.

The two main techniques to load thorium ions into RF trap s that have been employed so far, are using recoil ions from a uranium source[44] or laser ablation from a solid thorium compound like e.g., thorium nitrate (see, e.g., Refs. [37–39]). A uranium recoil source produces thorium ions of several charge states up to Th^{10+} or even higher[45,46]. However, the extracted charge state distribution is lowered by charge exchange when a buffer gas is used to reduce the initial kinetic energy. In the case of laser ablation, the produced charge state and number of ions strongly depend on the applied laser intensity and sample activity, with Th^{3+} being the highest charge state reached so far (see, e.g., Refs. [47,48]).

Solid-state samples

In 2003, Peik and Tamm suggested[7] that the favorable properties of the ^{229}Th isomer clock transition should persist even in a solid-state environment, sparking the idea of a "solid-state nuclear clock" that would make use of a dramatically higher particle number, possibly 10 or more orders of magnitude higher than in the trapped ion approach. ^{229}Th doping concentrations of $\sim 10^{17}$ cm^{-3} (corresponding to $\sim 0.01\%$ concentration) have been realized experimentally[49,50].

The ^{229}Th ions would be embedded (e.g., doped) into large band-gap crystal matrices, transparent in the vacuum-ultraviolet (VUV) range[7]. This system was analyzed theoretically and experimentally for a variety of host materials, mainly fluoride crystals such as CaF_2, MgF_2, LiCAF, LiSAF[51–53]. These samples serve as targets for attempts to directly excite the ^{229}Th isomer using synchrotron radiation, lasers, or X-ray pumping via higher-excited nuclear states[54].

Doping ^{229}Th into a single crystal is expected to lead to a Th^{4+} charge state, when the 4 valence electrons of neutral Th are bound by the surrounding crystal matrix. In most cases, this charge compensation locally modifies the crystal structure, creating vacancies or interstitial ions (mostly F^-). These defects (sometimes referred to as color centers) lead to the emergence of new electronic states within the band gap, spatially localized at the defect position. The involved electron wave functions have an overlap with the ^{229}Th nucleus and can lead to additional coupling mechanisms.

Previously regarded as a nuisance, these electronic defect states have recently been discussed as a means to populate, probe, or quench the isomeric state, in

loose analogy to electronic bridge mechanisms in ions[55]. Generally the nuclear coupling to these defect states is weak, not significantly altering the expected spontaneous decay rate for 4+ ions. However, they provide an intermediate level for 2-photon excitations, allowing to use powerful lasers at longer wavelength, and an increase in excitation rate by 2 orders of magnitude compared to direct radiative excitation has been conjectured for the Th:CaF$_2$ system. To date, these are theoretical considerations, as long as very little information about the microscopic structure of Th doping is available. Energy and linewidth of the defect states remains to be measured experimentally for different host materials.

Interaction of nuclear moments with the crystal fields leads to the emergence of level shifts, splittings, and broadenings[56,57]. All these effects need to be considered and quantified carefully in the design and operation of a solid-state-based nuclear clock. In particular, the nuclear quadrupole interaction with electric field gradients leads to the emergence of a nuclear quadrupole structure. The resulting level splittings are expected in the range of 50-500 MHz depending on the local field gradient at the position of the nucleus. They can be used for non-destructive state monitoring in nuclear quadrupole resonance spectroscopy and in schemes exploiting nuclear superradiance[58]. We find it interesting to note, that precision laser spectroscopy on the ^{229}Th nuclear transition in the solid-state would transfer the method of Mössbauer spectroscopy into the optical regime, maintaining the benefits of a recoil-free resonance line, and adding the advantages of using a coherent radiation source.

Transparent crystals are also used as implantation hosts for experiments using ^{229}Th recoil ions from external or internal ^{233}U sources[59,60], laser ablation plasmas[61], or ion beams from isotope facilities[31]. In contrast to doping, implantation samples leave the Th ions in an uncontrolled microscopic chemical environment. In general, crystal damage caused by the intrinsic Th radioactivity and exposure to the VUV or X-ray sources generate significant background signal[62], and effective suppression or filtering schemes need to be devised.

3. Measurements of the Thorium-229 isomer energy and nuclear moments

γ-ray measurements

The existence of the isomeric state in ^{229}Th was first deduced from the γ-ray spectroscopy of ^{233}U in 1976 (Ref. [9]). A consistent description of the observed γ-rays required the existence of an isomeric state, almost degenerate with the ground state. The experimental resolution of 450 eV allowed to place an upper bound on the isomer energy $E_{is} < 100$ eV. In a second experiment performed in 1985, several γ-ray energies in the range from 29 keV to 320 keV of ^{233}U → ^{229}Th α-decay were determined with a few eV precision[63]. These were used to obtain a more precise estimate of the isomer energy to be -1(4) eV (Ref.[64]).

An improved version of the experiment was performed in 1994 by the same group, and the isomer energy was determined to be 3.5(1.0) eV (Ref.[65]). This remained the accepted value for more than a decade, triggering a series of attempts to observe "nuclear fluorescence" from α-decaying ^{233}U directly. First claims of observation[66,67] were quickly identified as α-decay-induced fluorescence of nitrogen[68,69], as these experiments were performed in air. In 2005, the experimental data from Helmer and Reich were re-analyzed by including the effects of interband transitions, and the value of 5.5(1.0) eV for the isomer energy was obtained[70].

In 2007, a cryogenic microcalorimeter with 30 eV resolution was used to resolve the closely spaced transitions at 29.19 keV and 29.39 keV, as well as 42.43 keV and 42.63 keV (Refs.[30,71]). This allows extracting the isomer energy as:

$$E_{is} = (29.39 - 28.18 + 42.43 - 42.63) \text{ keV}$$

This method is less sensitive to the detector's energy calibration because only the energy differences of closely space transition are used. However, the authors did not report any systematic uncertainty, and it was argued that the actual uncertainty might be higher than quoted in the final result 7.8(5) eV (Refs.[29,72]). In 2019, a calorimetric experiment with FWHM = 40 eV reported the isomer energy to be 8.3(9) eV. This value is consistent with the previous reports but does not decrease the uncertainty.

The 29.19 keV and 42.43 keV lines are doublets with spacings equal to the isomer energy (see Fig. 3). A recent experiment using a cryogenic microcalorimeter with 10 eV resolution succeeded in resolving the 29.19 keV doublet for the first time[73]. The isomer energy can also be extracted directly from the splitting of the doublet lines. The isomer energy was found to be 8.10(17) eV using the double difference method (eq. 1) and 7.84(29) eV from the splitting of the 29.19 keV doublet. From the lineshape of the 29.19 keV doublet the improved value on the branching ratio was measured $b\left(\frac{29.19\ \mathrm{keV} \to 8\ \mathrm{eV}}{29.19\ \mathrm{keV} \to 0\ \mathrm{eV}}\right) = b_{29} = 9.3(6)\%$.
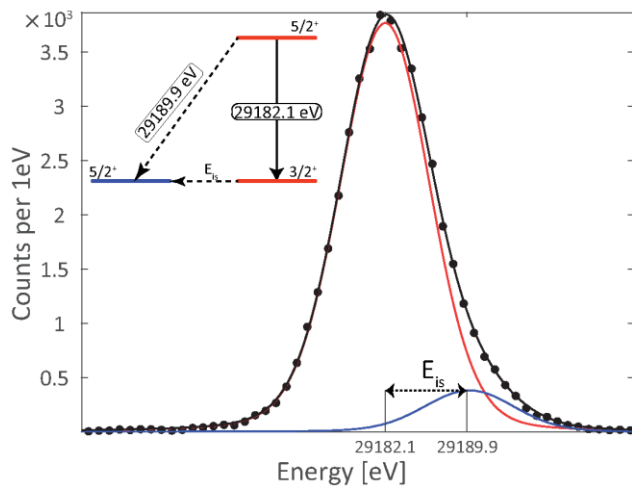

Fig. 3 | Lineshape of the 29.2 keV doublet[73]. The red curve represents the fit of the intraband $5/2^+ \to 3/2^+$ transition, and the blue curve represents the fit of the interband $5/2^+ \to 5/2^+$ transition. The black line is the sum of both transitions. Both the branching ratio and the isomer energy can be extracted directly from this fit. Inset: nuclear energy level diagram. The raw data is available in the Zenodo repository[121].

Internal conversion measurements

The first direct signature of the ^{229}Th isomer was obtained in 2016, about 30 years after first being predicted[74]. In this experiment, rather than the radiative decay of the isomer, internal conversion (IC) was detected. IC is a process in which the nuclear excitation energy is transferred to the electron shell, causing the ejection of a valence electron, which can then be detected[75].

The employed setup consisted of three parts: Production cell, filter, and detector. The production cell used a ^{233}U recoil source and a buffer gas stopping cell to slow down the energetic radioactive decay products and guide them towards an exit nozzle. All ^{233}U decay products are in an ionized state and can be filtered by a quadrupole mass spectrometer selecting for ^{229}Th, of which 2% are in the isomeric state. This filtered ion beam was directed to a microchannel plate (MCP), where the impacting ion created a "prompt" signal. Successively, the ion neutralizes by attracting electrons from the MCP metalized surface. While energetically forbidden for the ion, in the neutral ^{229}Th the excited nucleus can rapidly transfer its energy to a valence electron (IC), which creates a second signal on the detector, delayed by several microseconds[28].

To measure the energy of the ^{229}Th isomer, a magnetic bottle-type retarding field spectrometer[76] was added. The ions were now guided through a graphene foil, which neutralized them in-flight and triggered the IC process. The emitted electrons were magnetically guided towards a second MCP. A retardation voltage is used to measure the kinetic energy of the electrons. By combining the measured kinetic energy of the electrons with the remaining internal energy of Th, the isomer energy could be determined to be 8.28(17) eV. The uncertainty in this energy predominantly arises from unresolved distributions of initial and final electronic configurations of the ^{229}Th atom/ion in this process. The consistency of this result with the recent γ-measurements provides the desired confidence for building a dedicated VUV laser system for a nuclear clock in this wavelength region.

The success of using the IC process as a detection channel for the ^{229}Th isomer inspired a new experiment which is currently being prepared at UCLA & JILA. The concept is to combine narrow-band laser excitation with IC detection. In a recent proposal, it was shown that this combination could determine the nuclear clock transition frequency to 100 MHz precision using a VUV frequency comb[77].

Efforts are also underway to use a superconducting nanowire single photon detector (SNSPD) to replace the MCP plus magnetic bottle spectrometer to determine the isomer energy more accurately[78].

Electron shell spectroscopy: HFS measurements of nuclear moments

Due to the interaction between the nucleus and the electron shell, several nuclear parameters can be determined by performing precision spectroscopy on atomic transitions. The magnetic dipole moment µ and the electric quadrupole moment Q can be determined from the hyperfine splitting of electronic levels. A change of the mean squared charge radius r^2 between different isotopes and isomers can be measured by the relative isotope shift of these levels[7,79].

The magnetic dipole moment of the nuclear ground state of ^{229}Th has been measured in several experiments based on hyperfine spectroscopy[21,26,79]. The most precise value of $\mu = 0.360(7)\,\mu_N$ was obtained by precision spectroscopy of laser-cooled ^{229}Th^{3+} ions, combined with state-of-the-art atomic theory to calculate the electron wave function[26]. The same experiment also provided a measurement of the electric quadrupole moment $Q = 3.11(6)\,eb$, which agrees with an earlier value of $Q = 3.149(32)\,eb$ which was obtained via Coulomb excitation[80].

Experimental values $\mu = -0.37(6)\,\mu_N$ and $Q = 1.74(6)\,eb$ for the nuclear moments of the isomeric state were first obtained in 2018 by comparing the hyperfine structure of two electronic transitions in ^{229}Th^{2+} ions in ground (^{229g}Th) and isomeric (^{229m}Th) state, which were produced by a ^{233}U recoil source[25]. These values confirmed predictions for the quadrupole moment[81] and agree with current nuclear model calculations for the magnetic dipole moment[82,83]. The experiment in Ref. [25] also determined the change in mean squared charge radius between ^{229g}Th and ^{229m}Th as $<r_{229m}>^2-<r_{229g}>^2=0.012(2)\,fm^2$. This was achieved by comparing the isomeric shift of selected electronic transitions with their respective isotope shift between ^{232}Th and ^{229}Th. The result shows quantitatively that in the excitation to the isomeric state, not only an unpaired neutron, but also the proton distribution of ^{229}Th is affected.

By employing the parameters μ, Q, and r^2 of both nuclear states, the hyperfine structure of an electronic transition of the isomer can be predicted when the structure is known for the nuclear ground state (see Fig. 4 for a selected transition of Th^{3+}). This enables a highly efficient, non-demolition detection scheme for the isomeric state based on hyperfine spectroscopy, known as double resonance[7,84,85].
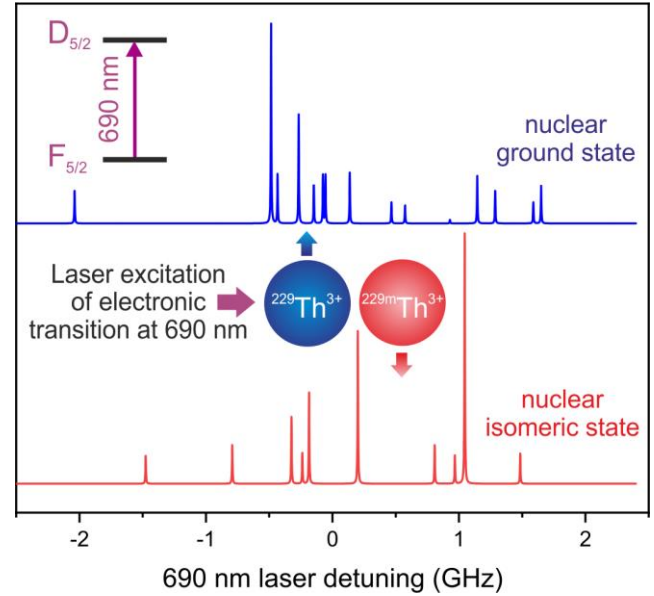

Fig. 4 | Simulated hyperfine structure of the F$_{5/2}$ → D$_{5/2}$ electronic transition at 690 nm in ^{229}Th^{3+} for the nuclear ground state (blue) and the isomer (red). The amplitudes are calculated assuming a uniform population of initial hyperfine states. The structures differ due to the difference in spin, nuclear moments, and mean squared charge radius between the two nuclear states[25,26]. This can be used to distinguish the two nuclear states via hyperfine spectroscopy.

4. Methods for exciting the Thorium-229 isomer

So far, all of the successful experiments described above used the α-decay of ^{233}U as a means to generate ^{229}Th in the isomeric state. While conceptually simple and reliable, this mechanism only has a 2% efficiency. Furthermore, it transfers 84 keV recoil energy to the "freshly born" ^{229}Th ion, often leaving it in an uncontrolled state concerning kinetics and charge.

More efficient and controlled methods of obtaining isomeric ^{229}Th are hence under investigation. These approaches can be coarsely divided into two main groups: one that exploits various coupling mechanisms between the electronic level structure and the nuclear ground and isomeric state, and one that uses light-induced transitions within the nuclear level structure only (see Figure 5). Both are briefly discussed in the following.
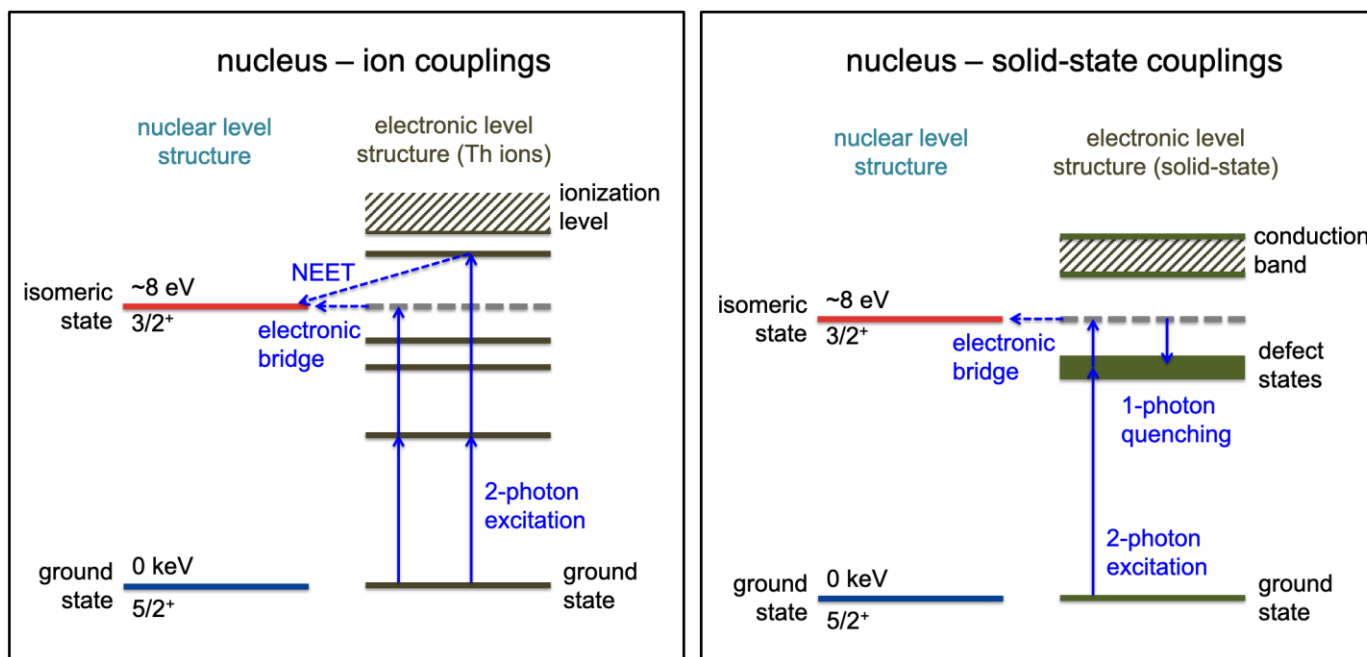
Fig. 5 | Left: Excitation schemes involving the [229]Th electronic level structure, shown here for ions in an ion trap or a plasma. The isomer can, e.g., be excited in a two-photon process by a resonant electronic bridge process, or via spontaneous emission from an excited electronic state (NEET). Right: Excitation and quenching schemes involving localized defect states emerging with Th dopant ions in a solid-state system. The isomer can be excited in a two-photon resonant electronic bridge process. Note that the intermediate defect state level is expected to be broad compared to electronic levels in free ions. A nuclear excitation can be quenched by shining in a single photon bridging between the nuclear and solid-state level.

Electronic bridge or NEET, LIEB excitation

The [229m]Th isomer has the unique property that its excitation energy is on the same order as processes of the outer-shell electrons. Interactions with the electron shell can, therefore, be expected to enhance the nuclear excitation and de-excitation rates significantly[86,87]. This can be employed to achieve excitation of the nucleus in a multi-photon process via nuclear excitation by electron transition (NEET) or the electronic bridge (EB) process[88,89].

The first attempt to excite a low-lying isomer by the NEET process was reported using a laser-produced plasma of [235]U in 1979 (Ref.[90]). A similar technique was proposed to obtain a large number of [229]Th isomeric nuclei[91], and a corresponding experimental attempt was performed in 2018 (Ref.[61]). Although the results of this work were not published in a reviewed journal, the excitation of the thorium isomer in a laser-produced plasma merits further investigation.

In the case of ionized thorium, the nuclear excitation energy lies below the ionization potential[92]. NEET/EB

excitation schemes are therefore concentrated on transitions between bound electronic states. In a scheme proposed for Th[+] ions, the electron shell is excited by two photons whose sum frequency equals the nuclear transition frequency, thereby coupling to the isomeric state[93].

Alternatively, it has been proposed to resonantly populate higher-lying electronic states in order to excite the nucleus in a two-photon decay process (see, e.g., Ref.[94]). Corresponding experiments are currently performed with trapped Th[+] and Th[2+] ions, which are characterized by their comparably high electronic level density in the energy range of the isomer[39,95,96].

Excitation via the electronic bridge process has also been proposed for highly charged Th[35+] ions in electron beam ion traps[97]. With increasing charge, fine-structure splittings in the electronic ground-state configuration become larger and eventually reach the value of the nuclear transition energy, at about the Th[35+] charge state. Since several fine-structure transitions with the same multipolarity as the nuclear transition are available, a highly efficient EB coupling can be expected.

In the case of the decay of the isomeric state, the laser-induced electronic bridge (LIEB) process can be used to achieve precise knowledge on the nuclear excitation energy[98]. In this scheme, a Th ion in the isomeric state is excited to a virtual electronic state. If this state is in resonance with an electronic excitation of the nuclear ground state, the nuclear decay is strongly enhanced. The nuclear excitation energy can then be inferred from the photon energy and the addressed electronic level.

Direct excitation of nuclear levels using synchrotron radiation

A series of attempts were made to resonantly excite the ^{229}Th nucleus from ground state to excited nuclear states using synchrotron or undulator sources of VUV light and to detect the ensuing fluorescence decay or other signals indicating successful excitation.

The first set of investigations focused on direct radiative excitation of the isomeric state. In 2014/15, Eric Hudson's group at UCLA used ^{229}Th-doped LiSrAlF$_6$ crystals (10^{16}-10^{17} cm^{-3} concentration) in the Advanced Light Source (ALS) synchrotron to optically excite the isomer[49]. ALS provided a 0.19 eV linewidth source with an integrated flux of ~7 x 10^{14} photons/s, tunable between 7.3 eV and 8.8 eV. A spectroscopic search for the nuclear resonance was performed during a 96 h run, scanning the interval in 0.1 eV steps with 2000 s illumination time. No nuclear fluorescence signal could be detected, which allowed to exclude (90% confidence level) short isomer lifetimes (between 1 - 2000 s) in the scanned energy interval. This assumes that non-radiative decay processes are negligible in the crystal.

A conceptually identical experiment was performed in 2017 at the Metrology Light Source (MLS) synchrotron[62]. This time around a ^{229}Th-doped CaF2 crystal (10^{16} cm^{-3} concentration) was used to scan for the isomer in the energy region 7.5-10 eV, again without success. A sample of surface-absorbed ^{229}Th nitrate on a CaF$_2$ carrier substrate has also been investigated at MLS in the energy range 3.9 - 9.5 eV (Ref.[99]). Again, no nuclear fluorescence signal could be detected.

These experiments highlight the need for a detailed understanding of the microscopic electronic structure and the relevance of non-radiative decay processes in solid-state samples.

A different approach consists of X-ray pumping via higher-excited nuclear states, using narrow-band synchrotron radiation. A pumping rate of 25 kHz into the isomeric state could recently be demonstrated in an experiment carried out at the SPring-8 synchrotron source, actively exciting ^{229}Th from the ground state into the 29 keV second excited state[54].

Resonant laser excitation

Towards the demonstration of a nuclear clock, the challenge remains to drive the nuclear excitation directly and resonantly with a narrow-band laser. The direct laser excitation of the ^{229}Th isomer is a complex task due to the current significant uncertainty in the nuclear transition energy, challenges of the laser radiation sources development and operation in the vacuum-ultraviolet (VUV) range. Development of dedicated laser systems for ^{229}Th nuclear spectroscopy is required, and underway in several groups worldwide.

Unfortunately, nonlinear optical crystals (NLO) for the generation of the VUV light in the wavelength range of the thorium isomer energy are still very scarce due to the strong absorption of the crystals in this wavelength region[100]. Currently, VUV light in the range of 150-156 nm has been obtained only in an optically contacted, prism-coupled KBe$_2$BO$_3$F$_2$ crystal (KBBF) by sum-frequency mixing of fundamental radiation and its fourth harmonic from pulsed Ti:sapphire laser systems[101,102]. The VUV output power achieved in the experiments with KBBF is much lower[101] than that for four-wave mixing based on third-order nonlinear interactions in a gas phase medium[103].
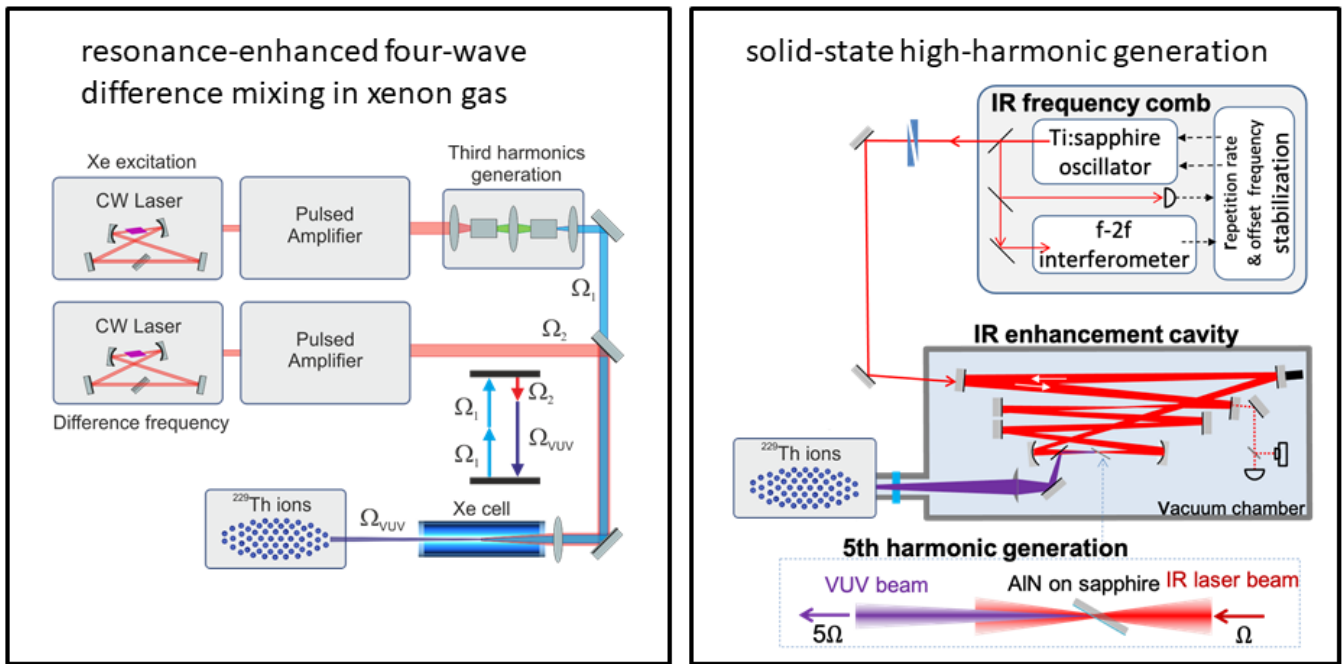
Fig. 6 | Left panel: VUV light for the resonant excitation of ^{229}Th is generated via four-wave-difference mixing by focusing laser radiation with the frequencies Ω_1 and Ω_2 into a xenon gas cell. High intensity pulses at Ω_1 and Ω_2 are produced by seeding two pulsed amplifiers with two CW lasers and subsequent frequency-tripling (in the case of Ω_1). The system can be used for interrogating the nuclear resonance of ^{229}Th ions in an ion trap or doped into a transparent host crystal. Right panel: Generation of 160 nm light as the 5th harmonic of an infrared (IR) 800 nm Ti:sapphire femtosecond frequency comb. The harmonic generation takes place in a passive enhancement cavity and uses a thin (30 microns) AlN layer as a target.

Sum- and difference-frequency conversion of pulsed laser radiation generates coherent tunable radiation in the VUV at wavelengths 60 – 200 nm (Ref.[104]).

A light source using resonance-enhanced four-wave difference mixing in xenon gas delivers high-intensity pulses of VUV light with a continuously tunable wavelength from 122 nm (10.2 eV) to 168 nm (7.4 eV)[105]. The VUV radiation intensity of the source is in the range of 10^{13} photons per 5 ns pulse for the wavelengths 150 - 160 nm. The linewidth of the VUV radiation and the pulse repetition rate of these sources is usually determined by pulsed amplifiers and lie in the range of hundreds of MHz and tens of Hz, respectively. Typical photon spectral densities of VUV radiation at 150 nm obtained in the four-wave mixing experiments are $\sim 10^6$ photons $\times$ sec^{-1} $\times$ Hz^{-1} which corresponds to ~ 1 pW $\times$ sec^{-1} $\times$ Hz^{-1} spectral power density. Because of the high spectral brightness, these VUV light sources are a useful tool for VUV spectroscopy of thorium.

Demonstrations of the generation of phase-coherent frequency combs in the VUV spectral region[106,107] open new frontiers of precision metrology[108] and development of optical clocks based on the nuclear transition in thorium. The excitation energy of the isomeric state corresponds to the 7th harmonic generation of a cavity-enhanced Yb-fibre frequency comb in xenon[109] or to the 5th harmonics of a frequency comb based on a Ti:sapphire laser. Thin films as a generation media of VUV light have recently attracted new attention because they require lower laser peak intensities than gases. Intense 5th harmonics generation of a Ti:sapphire laser is demonstrated recently from a thin AlN crystalline film grown on a sapphire substrate[110]. Typical continuous wave (CW) power of an individual VUV comb mode lies in the nW range depending on the laser source, the enhancement cavity, and the nonlinear medium. The linewidth of the individual mode depends on the phase and amplitude noise suppression of the laser source and varies for different comb systems. The linewidths

of the individual VUV modes generated by Yb-fiber combs were estimated in a few experiments to be in the range of 10 MHz[111,112]. In the assumption of a higher suppression of the laser phase noise and especially for the 5th harmonics of a Ti:sapphire optical comb, the linewidth of the individual comb mode in the range of 1 kHz might be within reach. Therefore, a spectral brightness of $\sim 10^7$ photons $\times$ sec^{-1} $\times$ Hz^{-1} might be obtained with VUV optical combs in the range of the thorium isomer energy, which is similar to four-wave mixing sources. Currently, until technology will offer suitable NLO crystals for VUV generation from CW lasers, we consider VUV optical frequency combs as the most promising light source for nuclear optical clock operation.

Assuming the spectral power density of the VUV source is in the order of 10^6 - 10^7 photons $\times$ sec^{-1} $\times$ Hz^{-1} and the beam waist of 100 μm, the excitation rate of the thorium isomeric state can be estimated (see, e.g., Ref. [113,114]) to be about $10^{-6} - 10^{-5}$ s^{-1} for an ion in an RF trap. For ^{229}Th ions doped into a solid, we expect the nuclear transition to be broadened to a linewidth of several kHz (Ref. [52]). This may increase the excitation yield due to increasing spectral overlap with the excitation source, but will ultimately degrade clock performance, once probed with a Hz-level laser system.

5) Performance of the nuclear clock and applications in fundamental physics

In view of applications in metrology, an important aspect of the ^{229}Th nuclear clock is the higher accuracy and robustness that it promises in comparison to optical clocks based on electronic transitions. In general, nuclear transition frequencies are less sensitive to external perturbations than transition frequencies in the electron shell because the nucleons are much more tightly bound, so that nuclear dimensions and nuclear moments are smaller (see Sect. 3). This advantage is especially important in the interaction with external electric fields. The smallness of the nuclear electric polarizability reduces frequency shifting effects of collisions with the background gas and the interaction with the thermal radiation emitted by all surfaces surrounding the atoms. If electronic and nuclear degrees of freedom could be decoupled, the nuclear transition frequency would be independent of

interactions that produce shifts of the electronic levels. While this is not possible for all orders of the hyperfine interaction, one may select a suitable electronic environment of the nucleus that minimizes the coupling to external perturbations. The choice may be made between electronic ground or metastable states of Th ions in various positive charge states, including Th^{3+} (favourable for trapped ion experiments), Th^{4+} (the dominant charge state of Th ions in solids) and also highly charged Th ions[97].

Two types of configurations have been identified where the hyperfine coupled nuclear transition frequency is immune against field-induced frequency shifts to a level that cannot be obtained for an electronic transition: (i) States with values 0 or ½ of electronic or total angular momenta J or F eliminate higher order and tensorial interactions[7]. (ii) Stretched states with aligned orientation of the electronic and nuclear angular momenta and maximum values of F and $|m_F|$ can be obtained for all values of J and are eigenstates in the coupled as well as in the uncoupled basis[8]. For the stretched states of the ^{229}Th^{3+} ground state it has been calculated that the relative frequency shift induced by thermal radiation at 300 K amounts to 1×10^{-22}, four to eight orders of magnitude smaller than in established atomic clocks.

At this level of suppression of field-induced frequency shifts, the dominant contributions to the uncertainty of a nuclear clock will be the relativistic Doppler shift from the motion of the nucleus, in the range of 10^{-18} or below for laser cooled ions, an effect that is common to all clocks, atomic and nuclear.

In the solid-state nuclear clock, the electronic degrees of freedom are more difficult to control and interactions with crystal fields cannot be fully avoided. In particular, the isomer shift will degrade the clock accuracy. On the upside, working with solid-state samples allows to interrogate up to 10^{15} nuclei deep in the Lamb-Dicke regime, which increases the clock precision. Performances of up to 10^{-19} relative clock stability were conjectured, but numerous questions on the interplay of the nuclear level structure with the microscopic crystal environment remain to be clarified[56,57].

A unique feature of the nuclear clock is its high sensitivity to possible phenomena of "new physics" beyond the Standard Model. Effects that would

potentially be observable with nuclear clocks are violations of Lorentz invariance, temporal variations of fundamental constants, or coupling to additional fields like dark matter. Such experiments have already been performed as Null tests at the limits of precision of the best atomic clocks, and a nuclear clock with higher sensitivity promises to advance the field[115].

The question of the sensitivity of the [229]Th nuclear clock to effects of "new physics" has stimulated interest in the underlying nuclear structure. Even without a detailed picture of the properties of the two nearly degenerate nuclear levels that are connected by the clock transition, some insight can be gained from intuitive considerations. In contrast to a transition in the electron shell, the nuclear transition energy is not purely electromagnetic but contains a contribution from the strong interaction. From the measured difference in the rms charge radius between isomer and ground state[25] a difference of Coulomb energy ΔE_C of about 100 keV between the two nuclear states can be inferred[116]. Given the small transition energy of 8 eV, it becomes clear that this change in Coulomb energy must be accompanied by a nearly equal but opposite change in the strong interaction energy. Because of this delicate balance, a hypothetical change in the value of the fine structure constant α would become apparent as a change in the transition frequency $\Delta f/f = (\Delta E_C/E_{ls}) \Delta\alpha/\alpha$ that is enhanced by about four orders of magnitude[85]. A similar reasoning can be applied to estimate the sensitivity to a change of the strong coupling constant[117,118] where variations conceivably could be stronger than for α. Even though the two interactions appear intertwined and the value of the $\Delta\alpha$-sensitivity cannot yet be predicted precisely, the nuclear clock promises to be a highly sensitive indicator for variations of fundamental constants. Recently the connection has been made that massive fields, such as dark matter, can produce an evolution of fundamental coupling constants of nature[119] and, again, the [229]Th nuclear clock could be the suitable detector.

Violations of Lorentz invariance would appear as an orientation dependence of the clock frequency where the sensitivity is determined by the anisotropy of the momentum distribution. The most sensitive experiment in the electron sector was a comparison of two Yb$^+$ single ion clocks[35]. A similar experiment with [229]Th nuclear clocks would allow one to study the neutron sector at high sensitivity[120]. Note that the neutron or proton momentum in a nucleus is more strongly relativistic ($v^2/c^2 \approx 10^{-3}$) than that of an atomic valence electron ($v^2/c^2 \approx \alpha^2 \approx 10^{-4}$).

Conclusion

Burdened with the complexity of a VUV laser system as the oscillator, the [229]Th nuclear clock is unlikely to find applications in the mundane domains of frequency metrology like telecommunication or navigation in the short term. One may also note that since the time when the [229]Th nuclear clock was first proposed in 2003, the demonstrated accuracy of optical atomic clocks has improved by more than three orders of magnitude. Notwithstanding the experimental difficulties and the strong competition, the prospects of the nuclear clock look as attractive as ever for opening a new field of research between atomic and nuclear physics and for novel opportunities for tests of fundamental physics. The recent advances in experimental methods for the preparation of [229]Th in different states as trapped ions or in solids and the now available precision data on its nuclear properties will facilitate the experimental progress and stimulate further conceptual ideas.

Data availability

The raw data for Fig. 3 are available in the Zenodo repository[121].

1. Pauli, W. Zur Frage der theoretischen Deutung der Satelliten einiger Spektrallinien und ihrer Beeinflussung durch magnetische Felder. *Naturwissenschaften* **12**, 741–743 (1924).

2. Casimir, H. Über die Hyperfeinstruktur des Europiums. *Physica* **2**, 719–723 (1935).

3. Rabi, I. I., Zacharias, J. R., Millman, S. & Kusch, P. A new method of measuring nuclear magnetic moment. *Physical Review* **53**, 318 (1938).

4. Laurence, W. Cosmic pendulum for clock planned. *New York Times* **34** (1945).

5. Ramsey, N. F. History of early atomic clocks. in *Metrologia* **42**, 1–3 (2005).

6. Ludlow, A. D., Boyd, M. M., Ye, J., Peik, E. & Schmidt, P. O. Optical atomic clocks. *Rev. Mod. Phys.* **87**, 637 (2015).

7. Peik, E. & Tamm, C. Nuclear laser spectroscopy of the 3.5 eV transition in Th-229. *Europhys. Lett.* **61**, 181–186 (2003).

8. Campbell, C. J. *et al.* Single-ion nuclear clock for metrology at the 19th decimal place. *Phys. Rev. Lett.* **108**, 120802 (2012).

9. Kroger, L. A. & Reich, C. W. Features of the low-energy level scheme of [229]Th as observed in the α-decay of 233U. *Nucl. Physics, Sect. A* **259**, 29–60 (1976).

10. Peik, E. & Okhapkin, M. *Nuclear clocks based on resonant excitation of γ-transitions*. *Comptes Rendus Physique* **16**, 516-523 (2015).

11. Thirolf, P. G., Seiferle, B. & von der Wense, L. The 229-thorium isomer: Doorway to the road from the atomic clock to the nuclear clock. *J. Phys. B At. Mol. Opt. Phys.* **52**, 203001 (2019).

12. Matinyan, S. Lasers as a bridge between atomic and nuclear physics. *Phys. Rep.* **298**, 199–249 (1998).

13. Tkalya, E. V. Properties of the optical transition in the 229 Th nucleus. *Physics-Uspekhi* **46**, 315–320 (2003).

14. Pálffy, A. Nuclear effects in atomic transitions. *Contemp. Phys.* **51**, 471 (2010).

15. von der Wense, L., Seiferle, B. & Thirolf, P. G. Towards a 229 Th-based nuclear clock. *Meas. Tech.* **60**, 13–22 (2018).

16. Peik, E., Zimmermann, K., Okhapkin, M. & Tamm, C. H. R. Prospects for a nuclear optical frequency standard based on thorium-229. in *Proceedings of the 7th Symposium on Frequency Standards and Metrology, ISFSM 2008* 532–538 (World Scientific Publishing Co. Pte Ltd, 2009).

17. von der Wense, L., Seiferle, B. The [229]Th isomer: prospects for a nuclear optical clock, *Eur. Phys. J. A* **56**, 277 (2020).

18. Varga, Z., Nicholl, A. & Mayer, K. Determination of the [229]Th half-life. *Phys. Rev. C - Nucl. Phys.* **89**, 1–6 (2014).

19. SRP thorium processing experience (Conference) | OSTI.GOV. Available at: https://www.osti.gov/biblio/6570656. (Accessed: 20th July 2020)

20. Forsberg, C. W. & Lewis, L. C. *Uses For Uranium-233: What Should Be Kept for Future Needs?* (1999).

21. Hogle, S. *et al.* Reactor production of thorium-229. *Appl. Radiat. Isot.* **114**, 19–27 (2016).

22. Egorov, V. N. Hyperfine structure of the atomic spectrum and the nuclear moments of the thorium-229 isotope. *Opt. Spectrosc.* **16**, 549-554 (1964)

23. Gulda, K., *et al.* The nuclear structure of [229]Th. *Nucl. Phys. A* **703**, 45–69 (2002).

24. Litvinova, E., Feldmeier, H., Dobaczewski, J. & Flambaum, V. Nuclear structure of lowest [229]Th states and time-dependent fundamental constants. *Phys. Rev. C* **79**, 064303 (2009).

25. Thielking, J. *et al.* Laser spectroscopic characterization of the nuclear-clock isomer [229m]Th. *Nature* **556**, 321 (2018).

26. Safronova, M. S., Safronova, U. I., Radnaev, A. G., Campbell, C. J. & Kuzmich, A. Magnetic dipole and electric quadrupole moments of the [229]Th nucleus . *Phys. Rev. A* **88**, 060501 (2013).

27. Minkov, N. & Pálffy, A. Reduced Transition Probabilities for the Gamma Decay of the 7.8 eV Isomer in ^{229}Th. *Phys. Rev. Lett.* **118**, 212501 (2017).

28. Seiferle, B., von der Wense, L. & Thirolf, P. G. Lifetime measurement of the ^{229}Th nuclear isomer. *Phys. Rev. Lett.* **118**, 042501 (2017).

29. Sakharov, S. L. On the energy of the 3.5-eV level in ^{229}Th. *Phys. At. Nucl.* **73**, 1–8 (2010).

30. Beck, B. R. *et al.* Energy splitting of the ground-state doublet in the nucleus ^{229}Th. *Phys. Rev. Lett.* **98**, 142501 (2007).

31. Verlinde, M. *et al.* Alternative approach to populate and study the ^{229}Th nuclear clock isomer. *Phys. Rev. C* **100**, 24315 (2019).

32. Kofoed-Hansen, O. On the Theory of the Recoil in β-Decay. *Phys. Rev.* **74**, 1785–1788 (1948).

33. Ferrer, R. *et al.* Towards high-resolution laser ionization spectroscopy of the heaviest elements in supersonic gas jet expansion. *Nat. Commun.* **8**, 1–9 (2017).

34. Paul, W. Electromagnetic traps for charged and neutral particles. *Reviews of Modern Physics* **62**, 531 (1990).

35. Sanner, C. *et al.* Optical clock comparison for Lorentz symmetry testing. *Nature* **567**, 204–208 (2019).

36. Brewer, S. M. *et al.* ^{27}Al$^+$ quantum-logic clock with a systematic uncertainty below 10^{-18}. *Phys. Rev. Lett.* **123**, 033201 (2019).

37. Kälber, W. *et al.* Nuclear radii of thorium isotopes from laser spectroscopy of stored ions. *Zeitschrift für Phys. A At. Nucl.* **334**, 103–108 (1989).

38. Campbell, C. J., Radnaev, A. G. & Kuzmich, A. Wigner crystals of ^{229}Th for optical excitation of the nuclear isomer. *Phys. Rev. Lett.* **106**, 223001 (2011).

39. Meier, D.-M. *et al.* Electronic level structure of Th$^+$ in the range of the ^{229m}Th isomer energy. *Phys. Rev. A* **99**, 52514 (2019).

40. Groot-Berning, K. *et al.* Trapping and sympathetic cooling of single thorium ions for spectroscopy. *Phys. Rev. A* **99**, 023420 (2019).

41. Herrera-Sancho, O. A. *et al.* Two-photon laser excitation of trapped ^{232}Th$^+$ ions via the 402-nm resonance line. *Phys. Rev. A - At. Mol. Opt. Phys.* **85**, 033402 (2012).

42. Feiock, F. D. & Johnson, W. R. Atomic susceptibilities and shielding factors. *Phys. Rev.* **187**, 39–50 (1969).

43. Schmidt, P. O. *et al.* Physics: Spectroscopy using quantum logic. *Science* **309**, 749–752 (2005).

44. von der Wense, L., Seiferle, B., Laatiaoui, M. & Thirolf, P. G. Determination of the extraction efficiency for ^{233}U source α-recoil ions from the MLL buffer-gas stopping cell. *Eur. Phys. J. A* **51**, 1–18 (2015).

45. Haas, R. *et al.* Development of a recoil ion source providing slow Th ions including $^{229(m)}$Th in a broad charge state distribution. *Hyperfine Interact.* **241**, 1–8 (2020).

46. Gunter, K., Asaro, F. & Helmholz, A. C. Charge and energy distributions of recoils from ^{226}Th alpha decay. *Phys. Rev. Lett.* **16**, 362–364 (1966).

47. Zimmermann, K., Okhapkin, M. V., Herrera-Sancho, O. A. & Peik, E. Laser ablation loading of a radiofrequency ion trap. *Appl. Phys. B Lasers Opt.* **107**, 883–889 (2012).

48. Campbell, C. J. *et al.* Multiply charged thorium crystals for nuclear laser spectroscopy. *Phys. Rev. Lett.* **102**, 233004 (2009).

49. Jeet, J. *et al.* Results of a direct search using synchrotron radiation for the low-energy ^{229}Th nuclear isomeric transition. *Phys. Rev. Lett.* **114**, 253001 (2015).

50. Stellmer, S. *et al.* Attempt to optically excite the nuclear isomer in ^{229}Th. *Phys. Rev. A* **97**, 062506 (2018).

51. Jackson, R. A., Amaral, J. B., Valerio, M. E. G., Demille, D. P. & Hudson, E. R. Computer modelling of thorium doping in LiCaAlF$_6$ and LiSrAlF$_6$: Application to the development of solid state optical frequency devices. *J. Phys. Condens. Matter* **21,** 325403 (2009).

52. Dessovic, P. *et al.* ^{229}Thorium-doped calcium fluoride for nuclear laser spectroscopy. *J. Phys. Condens. Matter* **26,** 105402 (2014).

53. Pimon, M. *et al.* DFT calculation of ^{229}thorium-doped magnesium fluoride for nuclear laser spectroscopy. *J. Phys. Condens. Matter* **32,** 255503 (2020).

54. Masuda, T. *et al.* X-ray pumping of the ^{229}Th nuclear clock isomer. *Nature* **573**, 238–242 (2019).

55. Nickerson, B. S. *et al.* Nuclear excitation of the ^{229}Th isomer via defect states in doped crystals. *Phys. Rev. Lett.* **125**, 032501 (2020).

56. Rellergert, W. G. *et al.* Constraining the evolution of the fundamental constants with a solid-state optical frequency reference based on the ^{229}Th Nucleus. *Phys. Rev. Lett.* **104**, 200802 (2010).

57. Kazakov, G. A. *et al.* Performance of a ^{229}Thorium solid-state nuclear clock. *New J. Phys.* **14** 083019 (2012).

58. Nickerson, B. S., Liao, W.-T. & Pálffy, A. Collective effects in ^{229}Th-doped crystals. *Phys. Rev. A* **98**, 062520 (2018).

59. Zhao, X. *et al.* Observation of the Deexcitation of the ^{229m}Th Nuclear Isomer. (2012). *Phys. Rev. Lett.* **109**, 160801 (2012).

60. Stellmer, S., Schreitl, M., Kazakov, G. A., Sterba, J. H. & Schumm, T. Feasibility study of measuring the ^{229}Th nuclear isomer transition with ^{233}U-doped crystals. *Phys. Rev. C* **94**, 14302 (2016).

61. Borisyuk, P. V. *et al.* Excitation of ^{229}Th nuclei in laser plasma: the energy and half-life of the low-lying isomeric state. arXiv:1804.00299 (2018).

62. Stellmer, S., Schreitl, M. & Schumm, T. Radioluminescence and photoluminescence of Th:CaF$_2$ crystals. *Sci. Rep.* **5**, 15580 (2015).

63. Reich, C. W., Helmer, R. G., Baker, J. D. & Gehrke, R. J. Emission probabilities and energies of of γ-ray transitions from the decay of ^{233}U. *Int. J. Appl. Radiat. Isot.* **35**, 185–188 (1984).

64. Reich, C. W. & Helmer, R. G. Energy separation of the doublet of intrinsic states at the ground state of ^{229}Th. *Phys. Rev. Lett.* **64**, 271–273 (1990).

65. Helmer, R. G. & Reich, C. W. An excited state of ^{229}Th at 3.5 eV. *Phys. Rev. C* **49**, 1845–1858 (1994).

66. Irwin, G. M. & Kim, K. H. Observation of electromagnetic radiation from deexcitation of the ^{229}Th isomer. *Phys. Rev. Lett.* **79**, 990–993 (1997).

67. Richardson, D. S., Benton, D. M., Evans, D. E., Griffith, J. A. R. & Tungate, G. Ultraviolet Photon Emission Observed in the Search for the Decay of the ^{229}Th Isomer. *Phys. Rev. Lett.* **80**, 3206–3208 (1998).

68. Shaw, R. W., Young, J. P., Cooper, S. P. & Webb, O. F. Spontaneous ultraviolet emission from ^{233}uranium/^{229}thorium samples. *Phys. Rev. Lett.* **82**, 1109–1111 (1999).

69. Utter, S. B. *et al.* Reexamination of the optical gamma ray decay in ^{229}Th. *Phys. Rev. Lett.* **82**, 505–508 (1999).

70. Guimarães-Filho, Z. O. & Helene, O. Energy of the 3/2$^+$ state of ^{229}Th reexamined. *Phys. Rev. C* **71**, 044303 (2005).

71. Beck, B. R. *et al.* Improved Value for the Energy Splitting of the Ground-State Doublet in the Nucleus ^{229}Th. LLNL-PROC-415170 (2009).

72. Kazakov, G. A., Schumm, T. & Stellmer, S. Re-evaluation of the Beck et al. data to constrain the energy of the Th-229 isomer. arxiv:1702.00749 (2017).

73. Sikorsky, T. *et al.* Measurement of the ^{229}Th isomer energy with a magnetic micro-calorimeter. *Phys. Rev. Lett.* **125**, 142503 (2020).

74. von der Wense, L. *et al.* Direct detection of the ^{229}Th nuclear clock transition. *Nature* **533**, 47–51 (2016).

75. Church, E. L. & Weneser, J. Nuclear structure effects in internal conversion. *Annu. Rev. Nucl. Sci.* **10**, 193–234 (1960).

76. Seiferle, B. *et al.* Energy of the ^{229}Th nuclear clock transition. *Nature* **573**, 243–246 (2019).

77. von der Wense, L. & Zhang, C. Concepts for direct frequency-comb spectroscopy of ^{229m}Th and an internal-conversion-based solid-state nuclear clock. *Eur. Phys. J. D* **74**, 146 (2020).

78. Seiferle, B. Characterization of the ^{229}Th nuclear clock transition. *PhD thesis, Ludwig-Maximilians Universität, München* (2019).

79. Gerstenkorn, S. *et al.* Structures hyperfines du spectre d'étincelle, moment magnétique et quadrupolaire de l'isotope 229 du thorium. *J. Phys.* **35**, 483–495 (1974).

80. Bemis, C. E. *et al.* Coulomb excitation of states in ^{229}Th. *Phys. Scr.* **38**, 657–663 (1988).

81. Tkalya, E. V. Proposal for a nuclear gamma-ray laser of optical range. *Phys. Rev. Lett.* **106**, 162501 (2011).

82. Dykhne, A. M. & Tkalya, E. V. Matrix element of the anomalously low-energy (3.5±0.5 eV) transition in ^{229}Th and the isomer lifetime. *JETP Lett.* **67**, 251–256 (1998).

83. Minkov, N. & Pálffy, A. Theoretical Predictions for the Magnetic Dipole Moment of ^{229m}Th. *Phys. Rev. Lett.* **122**, 162502 (2019).

84. Hayes, A. C., Friar, J. L. & Möller, P. Splitting sensitivity of the ground and 7.6 eV isomeric states of ^{229}Th. *Phys. Rev. C - Nucl. Phys.* **78**, 024311 (2008).

85. Berengut, J. C., Dzuba, V. A., Flambaum, V. V. & Porsev, S. G. Proposed experimental method to determine α sensitivity of splitting between ground and 7.6 eV isomeric states in ^{229}Th. *Phys. Rev. Lett.* **102**, 210801 (2009).

86. Porsev, S. G. & Flambaum, V. V. Electronic bridge process in ^{229}Th^{+}. *Phys. Rev. A - At. Mol. Opt. Phys.* **81**, 042516 (2010).

87. Karpeshin, F. F., Band, I. M. & Trzhaskovskaya, M. B. 3.5-eV isomer of ^{229m}Th: How it can be produced. *Nucl. Phys. A* **654**, 579–596 (1999).

88. Krutov, V. A. & Fomenko, V. N. Influence of Electronic Shell on Gamma Radiation of Atomic Nuclei. *Ann. Phys.* **476**, 291–302 (1968).

89. Morita, M. Nuclear excitation by electron transition and its application to uranium 235 separation. *Prog. Theor. Phys.* **49**, 1574–1586 (1973).

90. Izawa, Y. & Yamanaka, C. Production of ^{235}U^{m} by nuclear excitation by electron transition in a laser produced uranium plasma. *Phys. Lett. B* **88**, 59–61 (1979).

91. Strizhov, V. & Tkalya, E. Decay channel of low-lying isomer state of the. *Sov. physics, JETP* **72**, 387–390 (1991).

92. Herrera-Sancho, O. A., Nemitz, N., Okhapkin, M. V. & Peik, E. Energy levels of Th^{+} between 7.3 and 8.3 eV. *Phys. Rev. A - At. Mol. Opt. Phys.* **88**, 1–7 (2013).

93. Porsev, S. G., Flambaum, V. V., Peik, E. & Tamm, C. Excitation of the isomeric ^{229m}Th nuclear state via an electronic bridge process in ^{229}Th^{+}. *Phys. Rev. Lett.* **105**, 182501 (2010).

94. Müller, R. A., Volotka, A. V. & Surzhykov, A. Excitation of the ^{229}Th nucleus via a two-photon electronic transition. *Phys. Rev. A* **99**, 042517 (2019).

95. Meier, D. M. *Electronic level structure investigations in Th^{+} in the energy range of the ^{229}Th isomer.* PhD thesis, Leibniz University Hannover (2019).

96. Thielking, J. *Hyperfine studies of Th-229 in its nuclear ground and isomeric state.* PhD thesis Leibniz University Hannover (2020).

97. Bilous, P. V. *et al.* Electronic Bridge Excitation in Highly Charged ^{229}Th Ions. *Phys. Rev. Lett.* **124**, 192502 (2020).

98. Bilous, P. V., Minkov, N. & Pálffy, A. Electric quadrupole channel of the 7.8 eV ^{229}Th transition. *Phys. Rev. C* **97**, 044320 (2018).

99. Yamaguchi, A. *et al.* Experimental search for the low-energy nuclear transition in ^{229}Th with undulator radiation. *New J. Phys.* **17**, 053053 (2015).

100. Kang, L., Lin, Z., Liu, F. & Huang, B. Removal of A-site alkali and alkaline earth metal cations in KBe$_2$BO$_3$F$_2$-type layered structures to enhance the deep-ultraviolet nonlinear optical capability. *Inorg. Chem.* **57**, 11146–11156 (2018).

101. Kanai, T. *et al.* Generation of vacuum-ultraviolet light below 160 nm in a KBBF crystal by the fifth harmonic of a single-mode Ti:sapphire laser. *J. Opt. Soc. Am. B* **21**, 370 (2004).

102. Nakazato, T. *et al.* Phase-matched frequency conversion below 150 nm in $KBe_2BO_3F_2$. *Opt. Express* **24**, 17149 (2016).

103. Bjorklund, G. C. Effects of focusing on third-order nonlinear processes in isotropic media. *IEEE J. Quantum Electron.* **11**, 287–296 (1975).

104. Hilbig, R., Hilber, G., Lago, A., Wolff, B. & Wallenstein, R. Tunable coherent VUV radiation generated by nonlinear optical frequency conversion in gases. in *Nonlinear Optics and Applications* (ed. Yeh, P.) **0613**, 48 (SPIE, 1986).

105. Hanna, S. J. *et al.* A new broadly tunable (7.4-10.2 eV) laser based VUV light source and its first application to aerosol mass spectrometry. *Int. J. Mass Spectrom.* **279**, 134–146 (2009).

106. Gohle, C. *et al.* A frequency comb in the extreme ultraviolet. *Nature* **436**, 234–237 (2005).

107. Jones, R. J., Moll, K. D., Thorpe, M. J. & Ye, J. Phase-coherent frequency combs in the vacuum ultraviolet via high-harmonic generation inside a femtosecond enhancement cavity. *Phys. Rev. Lett.* **94**, 193201 (2005).

108. Witte, S., Zinkstok, R. T., Ubachs, W., Hogervorst, W. & Eikema, K. S. E. Deep-ultraviolet quantum interference metrology with ultrashort laser pulses. *Science* **307**, 400–403 (2005).

109. Yost, D. C. *et al.* Vacuum-ultraviolet frequency combs from below-threshold harmonics. *Nat. Phys.* **5**, 815–820 (2009).

110. Seres, J. *et al.* All-solid-state VUV frequency comb at 160 nm using high-harmonic generation in nonlinear femtosecond enhancement cavity. *Opt. Express* **27**, 6618-6628 (2019).

111. Cingöz, A. *et al.* Direct frequency comb spectroscopy in the extreme ultraviolet. *Nature* **482**, 68–71 (2012).

112. Ozawa, A. & Kobayashi, Y. Vuv frequency-comb spectroscopy of atomic xenon. *Phys. Rev. A - At. Mol. Opt. Phys.* **87**, 022507 (2013).

113. Hilborn, R. C. Einstein coefficients, cross sections, f values, dipole moments, and all that . *Am. J. Phys.* **50**, 982–986 (1982).

114. Cohen-Tannoudji, C. & Guéry-Odelin, D. *Advances in Atomic Physics: An Overview* (World Scientific, 2011).

115. Safronova, M. S. *et al.* Search for new physics with atoms and molecules. *Rev. Mod. Phys.* **90**, 025008 (2018).

116. Fadeev, P., Berengut, J. C. & Flambaum, V. V. Sensitivity of [229]Th nuclear clock transition to variation of the fine-structure constant. *Phys. Rev. A* **102**, 052833 (2020).

117. Flambaum, V. V. Enhanced effect of temporal variation of the fine structure constant and the strong interaction in [229]Th. *Phys. Rev. Lett.* **97**, 092502 (2006).

118. Flambaum, V. V. & Wiringa, R. B. Enhanced effect of quark mass variation in [229]Th and limits from Oklo data. *Phys. Rev. C* **79**, 034301 (2009).

119. Stadnik, Y. V. & Flambaum, V. V. Can dark matter induce cosmological evolution of the fundamental constants of nature? *Phys. Rev. Lett.* **115**, 201301 (2015).

120. Flambaum, V. V. Enhancing the effect of Lorentz invariance and Einstein's equivalence principle violation in nuclei and atoms. *Phys. Rev. Lett.* **117**, 072501 (2016).

121. Magnetic micro-calorimeter raw data | Zenodo. Available at: https://zenodo.org/record/3931904#.X5WqQYj7SUl. (Accessed: 25th October 2020).

Acknowledgements

Author contributions

The authors contributed equally to all aspects of the article.

Competing interests

The authors declare no competing interests